EVIDENCE FOR GLUON BREMSSTRAHLUNG IN e^+e^- ANNIHILATIONS AT HIGH ENERGIES

PLUTO Collaboration

Ch. BERGER, H. GENZEL, R. GRIGULL, W. LACKAS and F. RAUPACH
I. Physikalisches Institut der RWTH Aachen[1], *Germany*

A. KLOVNING, E. LILLESTÖL, E. LILLETHUN and J.A. SKARD
University of Bergen[2], *Norway*

H. ACKERMANN, G. ALEXANDER[3], F. BARREIRO, J. BÜRGER, L. CRIEGEE, H.C. DEHNE, R. DEVENISH[4], A. ESKREYS[5], G. FLÜGGE, G. FRANKE, W. GABRIEL, Ch. GERKE, G. KNIES, E. LEHMANN, H.D. MERTIENS, K.H. PAPE, H.D. REICH, B. STELLA[6], T.N. RANGA SWAMY[7], U. TIMM, W. WAGNER, P. WALOSCHEK, G.G. WINTER and W. ZIMMERMANN
Deutsches Elektronen-Synchrotron DESY, Hamburg, Germany

O. ACHTERBERG, V. BLOBEL[8], L. BOESTEN, H. KAPITZA, B. KOPPITZ, W. LÜHRSEN, R. MASCHUW[9], R. van STAA and H. SPITZER
II. Institut für Experimentalphysik der Universität Hamburg[1], *Germany*

C.Y. CHANG, R.G. GLASSER, R.G. KELLOGG, K.H. LAU, B. SECHI-ZORN, A. SKUJA, G. WELCH and G.T. ZORN[10]
University of Maryland[11], *Collegepark, MD, USA*

A. BÄCKER, S. BRANDT, K. DERIKUM, A. DIEKMANN, C. GRUPEN, H.J. MEYER, B. NEUMANN, M. ROST and G. ZECH
Gesamthochschule Siegen[1], *Germany*

T. AZEMOON[12], H.J. DAUM, H. MEYER, O. MEYER, M. RÖSSLER, D. SCHMIDT and K. WACKER[13]
Gesamthochschule Wuppertal[1], *Germany*

Received 13 September 1979

We report our results on the reactions $e^+e^- \to$ hadrons in the energy range $13 \leqslant E_{cm} \leqslant 31.6$ GeV and compare them with $q\bar{q}$ jets described in the quark–parton model and with first-order QCD predictions including gluon emission ($q\bar{q}g$ jets). At high energies the observed features of one-sided jet broadening, sea-gull effect and planar events with a three-jet structure represent a gross violation of the parton model without gluons and find a most natural interpretation if gluon bremsstrahlung is included.

[1] Supported by the BMFT, Germany
[2] Partially supported by the Norwegian Research Council for Science and Humanities
[3] On leave from Tel Aviv University, Israel
[4] Now at Oxford University, England
[5] On leave from Institute of Nuclear Physics, Krakow, Poland
[6] On leave from University of Rome, Italy; partially supported by INFN
[7] On leave from the Tata Institute, Bombay, India
[8] Now at CERN, Geneva, Switzerland
[9] Now at Technische Universität Karlsruhe, Germany
[10] University of Maryland General Research Board Grantee for 1978
[11] Partially supported by Department of Energy, USA
[12] Now at University College, London, England
[13] Now at Harvard University, Cambridge, Mass., USA

Several important attempts have been made recently to test specific predictions of quantum chromodynamics (QCD) [1] in hadron–hadron interactions [2], neutrino–hadron interactions [3], e^+e^- interactions at low energy [4] and the decay of the Υ meson [5,6]. Recently, first results have been reported on high-energy e^+e^- interactions observed at PETRA [7], which are the subject of this letter. In perturbative QCD (up to order α_s/π) the processes leading to hadronic final states [8] are

$$e^+e^- \to q\bar{q} \to \text{hadrons}, \quad (1)$$

$$e^+e^- \to q\bar{q}g \to \text{hadrons}. \quad (2)$$

At lower energies ($E_{cm} \lesssim 10$ GeV) the contribution of the gluon bremsstrahlung process (2) is expected to be negligible and the simple quark pair production process (1) with subsequent fragmentation into hadron jets with constant limited transverse momentum predominates. With increasing energy, however, reaction (2) becomes more and more important. Detailed predictions have been made recently [9,10] on how this effect influences the observable hadronic final state. In particular, a dramatic increase in $\langle p_\perp^2 \rangle$ as a result of one-sided jet broadening, planarity of events and finally an explicit three-jet structure are predicted.

In this letter we compare data taken at c.m. energies of 13, 17, 22, 27.6, 30 and 31.6 GeV with QCD predictions including the gluon bremsstrahlung process (2) and with the Field–Feynman model [11] of process (1) only. (For short we shall call the two models $q\bar{q}g$ and $q\bar{q}$.) Details of the experimental set up, the event selection criteria and the numbers of observed hadronic events are given in ref. [12] for the 13 and 17 GeV data and in the preceding letter [13] for the data at 22, 27.6, 30 and 31.6 GeV. Here we just want to emphasize again that the PLUTO detector is sensitive to charged (neutral) particles within 87% (94%) of the full solid angle.

To compare our data with the $q\bar{q}$ and $q\bar{q}g$ models we use two different Monte Carlo programs [‡1] to generate events which are subsequently passed through a complete detector simulation program and the same event recognition and analysis chain as used for the data. Initial state radiative effects are also included in the program. (All data presented in this letter are *observed* values. They are compared to Monte Carlo predictions which include both detector and radiative effects.) The $q\bar{q}$ generating program is based on the Field–Feynman model [11]. It contains u, d, s, c and b quarks and is sketched in the preceding letter [13]. The input parameter σ_q which determines the transverse momentum ($q_\perp$) distribution of the quark cascade $f(q_\perp) \sim \exp(-q_\perp^2/2\sigma_q^2)$ is fixed to the conventional value of $\sigma_q = 247.5$ MeV/c. For $q\bar{q}g$ the generating program was extended to allow for gluon bremsstrahlung of either q or $\bar{q}$. Following Hoyer et al. [10] gluons are radiated only by u, d, s, c quarks, gluon jets are treated as a combination of quark–antiquark pairs, the QCD cross section is taken for $q\bar{q}g$ but a cut-off on thrust is used. (This prescription yields a gluon jet in addition to the q and $\bar{q}$ jets in 15% (25%) of the generated events at 17 GeV (30 GeV) c.m. energy.)

In our data comparison with the $q\bar{q}$ and $q\bar{q}g$ predictions we first consider the averages $\langle p_\parallel \rangle$, $\langle p_\perp \rangle$ and $\langle p_\perp^2 \rangle$ computed from the hadron momenta parallel and perpendicular to the two-jet axis. We then study in detail one-sided jet broadening and finally demonstrate the occurrence of planar events as expected for $q\bar{q}g$.

Fig. 1 shows the averages $\langle p_\parallel \rangle$, $\langle p_\perp \rangle$ and $\langle p_\perp^2 \rangle$ computed for charged particles relative to the thrust axis of the event as a function of the c.m. energy. Here as in figs. 2–5 the axes are determined using both charged *and* neutral particles. The reason to compute $p_\parallel$ and $p_\perp$ only for charged particles is the following: In our shower counters we observe more clusters of deposited neutral energy than the expected number of neutral pions due to the decay $\pi^0 \to 2\gamma$. We treat all clusters as caused by photons. This should not influence the axis determination, especially not if linear methods like thrust [14] and triplicity [15] are used, but would give wrong results for the $p_\perp$ of π^0's. Fig. 1 shows that $\langle p_\parallel \rangle$ and $\langle p_\perp \rangle$ are not very discriminative between $q\bar{q}$ and $q\bar{q}g$, but the energy dependence of $\langle p_\perp^2 \rangle$ is better described if gluon bremsstrahlung is included.

To study this effect in more detail we distinguish for every event the two jets which are separated by a plane perpendicular to the thrust axis. The jet with the lower (higher) average $p_\perp$ is called the slim (fat) jet [9]. Fig. 2a shows $\langle p_\perp^2 \rangle$ of the charged particles as a function of the c.m. energy, where the average is taken over the charged hadrons in all slim (fat) jets. For the slim jet the $q\bar{q}$ and $q\bar{q}g$ predictions are very similar

[‡1] We are indebted to T. Meyer and H.G. Sander for providing essential parts of the Monte Carlo generators.

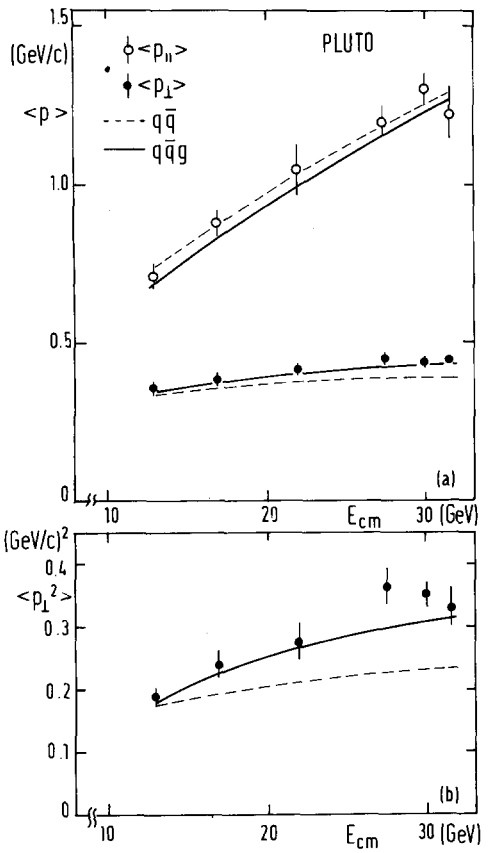

Fig. 1. Mean observed values of momentum components of charged particles parallel ($p_\parallel$) and perpendicular ($p_\perp$) to the thrust axis (a) and mean observed $p_\perp^2$ (b) as a function of the c.m. energy. The solid and dashed lines are $q\bar{q}g$ and $q\bar{q}$ predictions, respectively.

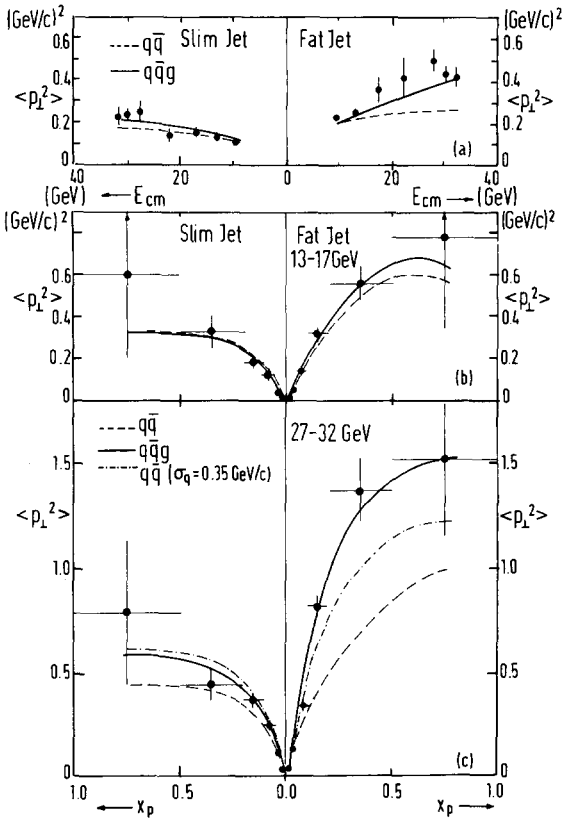

Fig. 2. Average observed $p_\perp^2$ of charged particles in the slim and fat jets, respectively, as a function of the c.m. energy (a). Sea-gull plots ($\langle p_\perp^2 \rangle$ of charged particles as a function of x_p) for slim and fat jets in two separate energy ranges (b), (c). The solid and dashed lines are $q\bar{q}g$ and $q\bar{q}$ predictions, respectively.

and the data are in agreement with both. For the fat jet, however, the data clearly favour $q\bar{q}g$, and $q\bar{q}$ is ruled out. We now turn to the question of which particles in the fat jet contribute most to the jet broadening. To answer this we construct the so-called "sea-gull plot" with the variables $x_p = p/p_{\text{beam}}$ (the normalized momentum) and $\langle p_\perp^2 \rangle$ computed from charged particles in a given x_p interval. We show it separately for slim and fat jets. To increase the statistical significance we group together the data at 13 and 17 GeV (fig. 2b) and at 27.6, 30 and 31.6 GeV (fig. 2c). (We have checked in separate plots for all five energies that this procedure is legitimate.) At the lower energy there is very little difference between $q\bar{q}$ and $q\bar{q}g$ predictions. The difference between the sea-gull plots for slim and fat jets can be explained by statistical fluctuations in the individual events. For the higher energies, however, $q\bar{q}g$ predicts a genuine one-sided jet broadening caused by the additional gluon jet. This effect is quite dramatic, especially at high x_p. It is observed in the data and cannot be explained by $q\bar{q}$. As a check we also ran the $q\bar{q}$ Monte Carlo with σ_q increased artificially to 350 MeV (dotted line in fig. 2c) but were unable to fit the data.

Now that we have shown that the data display the one-sided jet broadening expected from $q\bar{q}g$ we search for events with a three-jet structure. To this end we use the triplicity method [15]. The final state hadrons with the momenta $\boldsymbol{p}_1, \boldsymbol{p}_2, \ldots, \boldsymbol{p}_N$ are grouped into three nonempty classes C_1, C_2, C_3 with the total momenta

$$P(C_l) = \sum_{i \in C_l} \boldsymbol{p}_i , \quad l = 1, 2, 3 . \tag{3}$$

Triplicity is defined [‡2] by:

$$T_3 = \left(1 \Big/ \sum_{i=1}^{N} |\boldsymbol{p}_i|\right) \times \max_{C_1, C_2, C_3} \{|\boldsymbol{P}(C_1)| + |\boldsymbol{P}(C_2)| + |\boldsymbol{P}(C_3)|\} . \tag{4}$$

It ranges between $T_3 = 1$ for a perfect three-jet and $T_3 = 3\sqrt{3}/8 = 0.65$ for a perfectly spherical event. The classes C_l^* of particles yielding the maximum T_3 are identified with the hadron jets (fig. 3a) formed by the three quanta q, $\bar{q}$ and g. Thus the jet momenta are $\boldsymbol{P}(C_l^*)$. We rename them $\boldsymbol{P}_1, \boldsymbol{P}_2, \boldsymbol{P}_3$ with the convention $P_1 \geqslant P_2 \geqslant P_3$. Because of momentum conservation these vectors are coplanar and span the "triplicity plane". The angles between the jets (fig. 3b) can be interpreted as the angles between the quanta. Because of $\theta_1 + \theta_2 + \theta_3 = 360°$ [‡3] one can span a triangular Dalitz plot of which only 1/6 is populated (shaded area in fig. 3c) since $\theta_1 \leqslant \theta_2 \leqslant \theta_3$. The three corners A, B, C correspond to the totally symmetric three-jet case (A: $\theta_1 = \theta_2 = \theta_3 = 120°$) and two two-jet-like configurations (B: $\theta_1 = 0°, \theta_2 = \theta_3 = 180°$; C: $\theta_3 = 180°$, $\theta_1 = \theta_2 = 90°$, $P_3 = 0$). The event shown in fig. 4 demonstrates that planar events with a three-jet structure are in fact recognized by the triplicity method.

In fig. 3d we show a scatter diagram for triplicity versus thrust for all events in the high-energy region between 27.4 and 31.6 GeV. In this plot three-jet events are concentrated in a band of large triplicity, say $T_3 > 0.9$. Two-jet events have a large thrust. They are located in the upper right corner of the diagram. (We cannot distinguish between two-jet and three-jet

[‡2] It should be noted that thrust [14] is defined analogously by partition of the momenta into two classes only. It is then also clear that for every event $T_3 \geqslant T$.

[‡3] In the measured events momentum is not exactly conserved because of measurement errors and particle losses. Therefore, for the purpose of fig. 3e a "missing momentum vector" was added.

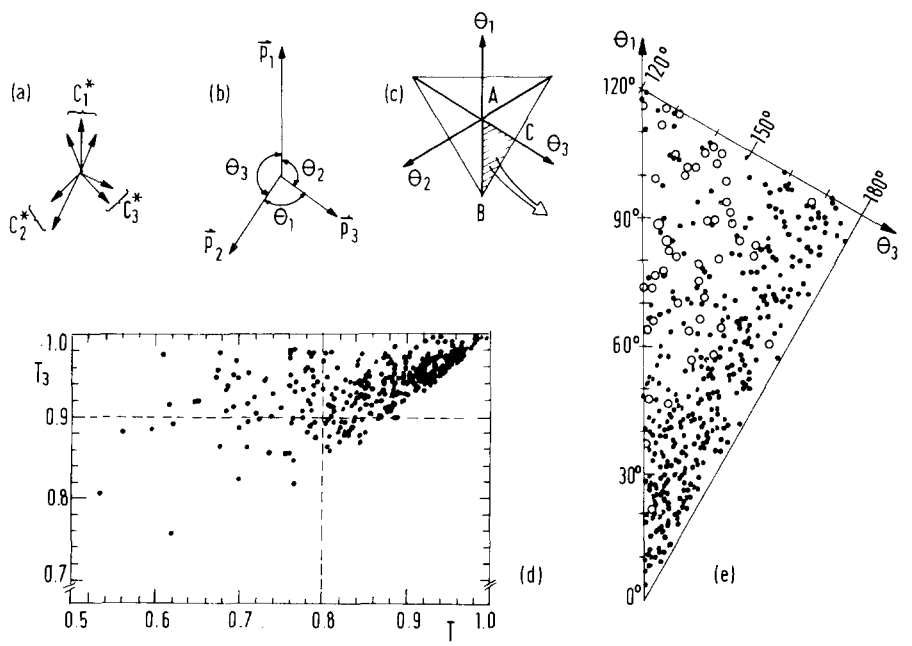

Fig. 3. Momentum configuration of hadrons (a) and jets (b) obtained by grouping hadrons into three classes according to the triplicity method. A Dalitz plot (c) can be spanned by the angles between the jets whose shaded area only is populated. Nearly symmetrical three-jet events will be situated near point A. The data at $E_{cm} = 27.6$, 30 and 31.6 GeV are shown in a scatter diagram of triplicity versus thrust (d) and in the angular Dalitz plot (e). In (d) planar events will be in the upper left of the plot characterized by low thrust and high triplicity, e.g., $T < 0.8$ and $T_3 > 0.9$. Events falling in this category show up as large circles in (e).

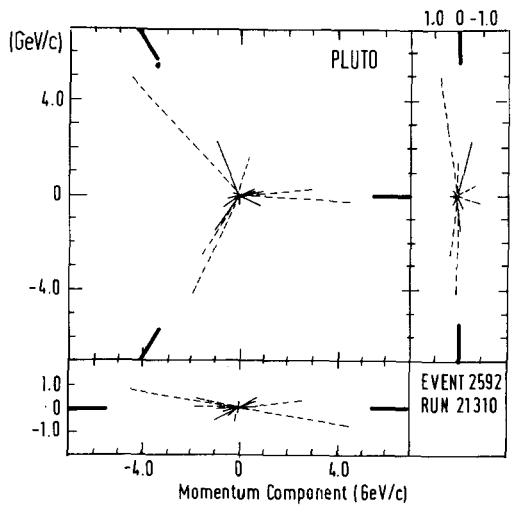

Fig. 4. Momentum vectors of an event (E_{cm} = 31.6 GeV) with high triplicity and low thrust projected onto the triplicity plane (top left), onto a perpendicular plane normal to the fastest jet (top right) and onto a plane containing the direction of the fastest jet (bottom). Solid and dotted lines correspond to charged and neutral particles, respectively. The directions of the jet axes are indicated as fat bars near the margins of the figures.

events at very high thrust.) For approximately spherical events both thrust and triplicity are low. In table 1 we give the number of three-jet events (defined by $T_3 > 0.9$, $T < 0.8$) and the numbers expected from $q\bar{q}$ and $q\bar{q}g$ for the two energy intervals. At the higher energies we observe 48 events, 43 are predicted by $q\bar{q}g$ but only 11 by $q\bar{q}$. The predictions from both models agree, however, with the lower-energy data.

The angular Dalitz plot for the high-energy events is shown in fig. 3e. The three-jet events as defined by the cuts in fig. 3d are drawn as large circles, the others as small dots. In this plot events with a conspicuous three-jet structure will appear near point A, i.e., for θ_3 significantly less than 180°. Table 1 contains the number of events observed and expected for $\theta_3 < 150°$ for the low- and high-energy samples. Again at high energies the data are consistent with $q\bar{q}g$ only. We conclude from this observation that indeed a three-jet event structure develops with increasing energy as predicted by the $q\bar{q}g$ model.

Independent of this study we also looked simply at the planarity of the events using the method we already employed in our analysis of the Υ decay [5]. We construct the conventional sphericity tensor [16]

$$T^{\alpha\beta} = \sum_{i=1}^{N} (p_i^2 \delta^{\alpha\beta} - p_i^{\alpha} p_i^{\beta}), \qquad (5)$$

where the $\boldsymbol{p}_i$ are the momentum vectors of all (charged and neutral) hadrons and α, β are the coordinate indices. We now order the eigenvalues λ_k of $T^{\alpha\beta}$ so that $\lambda_1 \geqslant \lambda_2 \geqslant \lambda_3$ and call the corresponding eigenvectors $\hat{\boldsymbol{n}}_1, \hat{\boldsymbol{n}}_2, \hat{\boldsymbol{n}}_3$. The sphericity axis is $\hat{\boldsymbol{n}}_3$. If the events are disk-like the normal to the disk plane is $\hat{\boldsymbol{n}}_1$. The vector $\hat{\boldsymbol{n}}_2$ lies in the disk plane and is normal to the sphericity axis. We now form the averages $\langle p_{out}^2 \rangle = \langle (\boldsymbol{p} \cdot \hat{\boldsymbol{n}}_1)^2 \rangle$ and $\langle p_{in}^2 \rangle = \langle (\boldsymbol{p} \cdot \hat{\boldsymbol{n}}_2)^2 \rangle$ over all charged particles of an

Table 1
Observed and expected numbers of events obeying different selection criteria.

E_{cm} (GeV)	Selected region	Events observed	Events expected (σ_q = 250 MeV/c)		Events expected (σ_q = 300 MeV/c)		Events expected (σ_q = 350 MeV/c)
			$q\bar{q}$	$q\bar{q}g$	$q\bar{q}$	$q\bar{q}g$	$q\bar{q}$
13–17	$T_3 > 0.9$, $T < 0.8$ (three-jet events)	24	11	15	15.5	17.5	20
	$\theta_3 < 150°$	32	25	32	27	33	29
	$\langle p_{in}^2 \rangle > 0.5$ GeV$^2/c^2$	5	5	5	7	10	9
	$S > 0.25$, $Q_1 < 0.03$ (planar events)	7	8	8	9	9	11
27–32	$T_3 > 0.9$, $T < 0.8$ (three-jet events)	48	11	43	23.5	48.5	36
	$\theta_3 < 150°$	52	19	51	25	50	31
	$\langle p_{in}^2 \rangle > 0.5$ GeV$^2/c^2$	68	23	56	30	61	37
	$S > 0.25$, $Q_1 < 0.03$ (planar events)	35	12	30	17	30	22

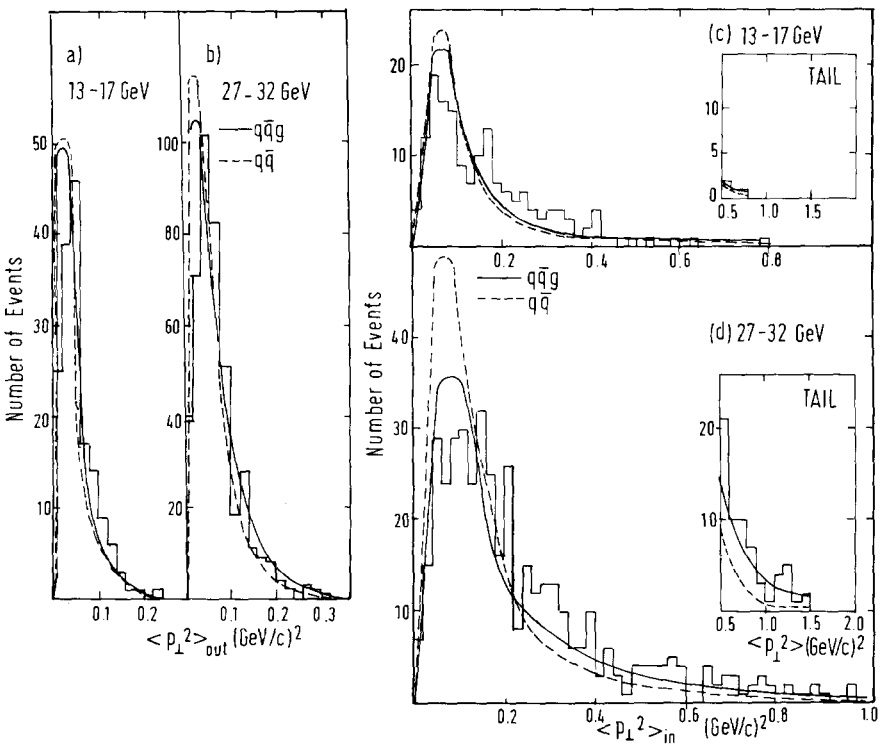

Fig. 5. Distributions of $\langle p^2_{\mathrm{out}}\rangle$ and $\langle p^2_{\mathrm{lin}}\rangle$ for the lower- and higher-energy regions. Solid and dashed lines are $q\bar{q}g$ and $q\bar{q}$ predictions, respectively.

event as a measure of the momentum out of the plane and in the plane in a direction perpendicular to the sphericity axis. Fig. 5 shows the distributions of $\langle p^2_{\mathrm{out}}\rangle$ and $\langle p^2_{\mathrm{lin}}\rangle$ for the two energy regions and for comparison of the predictions of $q\bar{q}g$ and $q\bar{q}$. We observe that at high energies the $\langle p^2_{\mathrm{lin}}\rangle$ distribution develops a tail. This tail corresponds to planar events which are predicted by $q\bar{q}g$ but cannot be accounted for by $q\bar{q}$. Table 2 contains the mean values of $\langle p^2_{\mathrm{out}}\rangle$ and $\langle p^2_{\mathrm{lin}}\rangle$ at two energies, in table 1 we give the number of events observed and expected for $\langle p^2_{\mathrm{lin}}\rangle > 0.5$ GeV$^2/c^2$. At the higher energies we observe 68 events, $q\bar{q}g$ predicts 56 whereas only 23 are expected from $q\bar{q}$. If we use only charged particles in the determination of the tensor (5) the distributions become slimmer and the tails shorter in data and Monte Carlo predictions but the conclusions do not change. (We have also studied the distributions of $\langle p^2_{\mathrm{out}}\rangle$ and $\langle p^2_{\mathrm{lin}}\rangle$ computed with respect to the normal to the triplicity plane and with respect to a unit vector in the triplicity plane perpendic-

Table 2
Observed and predicted mean values of $\langle p^2_{\mathrm{lin}}\rangle$ and $\langle p^2_{\mathrm{out}}\rangle$.

E_{cm} (GeV)	Variable (GeV/c)^2	Observed value	Predicted value (σ_q = 250 MeV/c)		Predicted value (σ_q = 300 MeV/c)		Predicted value (σ_q = 350 MeV/c)
			$q\bar{q}$	$q\bar{q}g$	$q\bar{q}$	$q\bar{q}g$	$q\bar{q}$
13–17	$\langle\langle p^2_{\mathrm{lin}}\rangle\rangle$	0.17 ±0.01	0.13	0.13	0.16	0.17	0.20
	$\langle\langle p^2_{\mathrm{out}}\rangle\rangle$	0.055 ±0.003	0.050	0.050	0.057	0.060	0.065
27–32	$\langle\langle p^2_{\mathrm{lin}}\rangle\rangle$	0.290 ±0.06	0.176	0.276	0.21	0.30	0.250
	$\langle\langle p^2_{\mathrm{out}}\rangle\rangle$	0.076 ±0.003	0.067	0.076	0.077	0.086	0.086

ular to the fastest jet axis, respectively. The results are very similar to those shown in fig. 5. However, all distributions are somewhat broader, since diagonalization of (5) minimizes $p_\perp^2$ with respect to $\hat{n}_3$ whereas (4) maximizes $p_\parallel$ with respect to the three-jet axis.)

Planar events can also be defined by using the quantities [5]

$$Q_k = 1 - 2\lambda_k/(\lambda_1 + \lambda_2 + \lambda_3) = \sum_{i=1}^{N} (\boldsymbol{p}_i \cdot \hat{\boldsymbol{n}}_k)^2 \Big/ \sum_{i=1}^{N} p_i^2 . \quad (6)$$

Because of $Q_1 + Q_2 + Q_3 = 1$ every event can be represented as a point in a Dalitz-like triangle spanned by the Q's [5]. Events with small $\langle p_{\text{out}}^2 \rangle$ are characterized by small Q_1 because $\langle p_{\text{out}}^2 \rangle = \langle (\boldsymbol{p} \cdot \hat{\boldsymbol{n}}_1)^2 \rangle$. Since two-jet events have small sphericity $S = 3\lambda_3/(\lambda_1 + \lambda_2 + \lambda_3) = (3/2)(Q_1 + Q_2)$, planar events [‡4] can be selected by requiring S to be large and Q_1 to be small. The number of planar events (defined by $S > 0.25$, $Q_1 < 0.03$) is given in table 1 together with $q\bar{q}$ and $q\bar{q}g$ expectations for the two energy regions. For the high energies the observed number can only be explained by $q\bar{q}g$.

We have tried both the $q\bar{q}$ and the $q\bar{q}g$ model increasing the value of σ_q to 300 MeV/c (as compared to the conventional value of σ_q = 250 MeV/c). The results obtained are similar and listed in the second and third column from the left in tables 1 and 2. As before the data rule out $q\bar{q}$ and favour $q\bar{q}g$. Increasing σ_q the $q\bar{q}g$ model reproduced slightly better the low end of the $\langle p_{\perp\text{in}}^2 \rangle$ distribution. However, we do not find this a compelling reason to abandon the original Field–Feynman value of σ_q = 250 MeV/c which so far has fit the data well over a wide energy region.

Finally, we have tried a $q\bar{q}$ model with an energy-dependent σ_q, even though no physical reason may be given for such an energy dependence in the framework of the Field–Feynman model. In order to reproduce the inclusive $p_\perp^2$ distribution we have to choose σ_q = 300 MeV/c at 17 GeV and σ_q = 350 MeV/c at 30 GeV. The latter yields the observed value of $\langle p_\perp \rangle$ = 450 MeV/c. But even with this artificially increased σ_q the $q\bar{q}$ model is unable to explain many features of our data, such as the sea-gull effect (dotted line in fig. 2c) and the number of three-jet events, planar events and events in the tail of the $\langle p_{\perp\text{in}}^2 \rangle$ distribution (last column in tables 1 and 2).

We conclude that for $E_{\text{cm}} \approx 30$ GeV the data do not agree with the simple $q\bar{q}$ model. At the same time the data are very well described by perturbative QCD taking into account gluon bremsstrahlung. This model accounts for the observed one-sided jet broadening and the asymmetric sea-gull effect as well as the planar configuration of the events having a three-jet structure.

We gratefully acknowledge the outstanding efforts of the PETRA machine group to push the storage ring to higher energies. We are also indebted to the technicians of the service groups who supported the experiment during data taking, namely our cryogenic group, the computer center, the gas supply group, the vacuum group, and the Hallendienst. We thank our technicians for the construction and maintenance of the PLUTO detector. We are grateful for discussions with members and guests of the DESY theory group. The non-DESY members of the collaboration want to thank the DESY directorate for support and hospitality extended to them.

References

[1] H. Fritzsch, M. Gell-Mann and H. Leutwyler, Phys. Lett. 47B (1973) 365;
D.J. Gross and F. Wilczek, Phys. Rev. Lett. 30 (1973) 1343;
H. Politzer, Phys. Rev. Lett. 30 (1973) 1346; Phys. Rep. 14C (1974) 129; Phys. Lett. 70B (1977) 430.

[2] C. Bromberg et al., Phys. Rev. Lett. 43 (1979) 565.

[3] J.G.H. de Groot et al., Phys. Lett. 82B (1979) 292, 456; Z. Phys. C1 (1979) 143;
P.C. Bosetti et al., Nucl. Phys. B149 (1979) 13.

[4] S.I. Eidelman et al., Phys. Lett. 82B (1979) 278.

[5] PLUTO Collab., Ch. Berger et al., Phys. Lett. 82B (1979) 449.

[6] PLUTO Collab., Ch. Berger et al., Talk presented by S. Brandt at the Intern. Conf. on High energy physics (Geneva, 27 June–4 July 1979), to be published; and DESY 79/43.

[7] TASSO Collab., Talks presented by R. Cashmore, P. Söding and G. Wolf at the Intern. Conf. on High energy physics (Geneva, 27 June–4 July 1979), to be published, and DESY 79/53;
PETRA Groups (JADE-Collab. (talk by S. Orito), MARK-J Collab. (talk by N. Newman), PLUTO Collab. (talk by Ch. Berger), TASSO Collab. (talk by G. Wolf)), presented to the Intern. Symp. on Lepton and photon interactions at high energies (FNAL, 23–29 Aug. 1979).

‡4 A slightly different definition of planarity is given in ref. [17].

[8] J. Ellis, M.K. Gaillard and G. Ross, Nucl. Phys. B111 (1976) 253;
T.A. DeGrand, Y.J. Ng and S.-H.H. Tye, Phys. Rev. D16 (1977) 3251.
[9] A. de Rujula et al., Nucl. Phys. B138 (1978) 387;
G. Kramer and G. Schierholz, Phys. Lett. 82B (1979) 108.
[10] P. Hoyer, P. Osland, H.G. Sander, T.F. Walsh and P.M. Zerwas, DESY 79/21, to be published.
[11] R. Field and R.P. Feynman, Nucl. Phys. B136 (1978) 1.
[12] PLUTO Collab., Ch. Berger et al., Phys. Lett. 81B (1979) 410.
[13] PLUTO Collab., Ch. Berger et al., preceding letter.
[14] S. Brandt, Ch. Peyrou, R. Sosnowski and A. Wroblewski, Phys. Lett. 12 (1964) 57;
E. Farhi, Phys. Rev. Lett. 39 (1977) 1587.
[15] S. Brandt and H.D. Dahmen, Z. Phys. C1 (1979) 61.
[16] J.D. Bjorken and S.J. Brodsky, Phys. Rev. D1 (1970) 1416.
[17] G. Knies, Proc. XIVth Rencontre de Moriond (1979), to be published, and DESY 79/47.